Development of Hardware-in-the-loop Microgrid Testbed

Bailu Xiao, Michael Starke, Guodong Liu, Ben Ollis, Philip Irminger, and Aleksandar Dimitrovski
Power & Energy Systems Group
Oak Ridge National Laboratory
Oak Ridge, USA

Kumaraguru Prabakar, Kevin Dowling, and Yan Xu
Dept. of Electrical Engineering and Computer Science
The University of Tennessee
Knoxville, USA

***Abstract*— A hardware-in-the-loop (HIL) microgrid testbed for the evaluation and assessment of microgrid operation and control system has been presented in this paper. The HIL testbed is composed of a real-time digital simulator (RTDS) for modeling of the microgrid, multiple NI CompactRIOs for device level control, a prototype microgrid energy management system (MicroEMS), and a relay protection system. The applied communication-assisted hybrid control system has been also discussed. Results of function testing of HIL controller, communication, and the relay protection system are presented to show the effectiveness of the proposed HIL microgrid testbed.**

I. INTRODUCTION

The rapid development of renewable energy applications leads to a large number of research works on microgrid, which is one of the most effective forms for grid integration of distributed energy resources (DERs) [1], [2]. The microgrid can be operated in grid-connected mode or islanded mode, which helps to mitigate the adverse effects of renewable energy resources and improve the reliability and energy efficiency of the grid. This unique feature of microgrid requires new coordinated control algorithms, energy management system, and protection schemes [3]-[5].

While computer simulations can be used to analyze and verify many concepts and schemes related to microgrid, those computer models become very complicated when the entire microgrid is simulated at full dynamic order. In addition, computer simulations have limitations on microgrid study, especially on those issues related to communication and protection. Thus, a microgrid testbed embedded with different DERs has been proposed as a powerful evaluation tool and helpful in promoting the development of microgrid research. There are many microgrid testbeds and demonstration projects built in different countries. In US, CERTS microgrid testbed, which consists of three feeders with loads and three microsources, has been built and operated by American Electric Power. It successfully demonstrated the ease of integrating distributed energy sources into a microgrid [6]. The University of California, San Diego (UCSD) has developed a 42 MW university microgrid with a master controller and optimization system that creates a self-sustaining campus [7]. Various researches have been conducted on optimization algorithms and predictive analytics related to microgrid. In Europe, within the frame of the European project "Microgrid" several microgrid testbeds have been installed. Take the DeMoTec at ISET as an example, it mainly focuses on electrification with renewable energies using modularly expandable and grid-compatible hybrid power supply systems [8]. The latest R&D findings and products related to the generation or consumption of electrical energy can be demonstrated. These testbeds provide experimental platforms for microgrid research. However, it is difficult to evaluate strategies and carry out testing under various scenarios and events. Since these testbeds usually involve a fixed hardware configuration, which is time consuming and costly to reconfigure. And the experiments are dependent on local weather and environment conditions.

Thus, hardware-in-the-loop (HIL) techniques can be introduced to the microgrid testbed [9]-[11]. By combining the HIL techniques and computationally advanced real-time systems, the flexibilities of both the microgrid testbed and its test conditions can be improved significantly. In this paper, a real-time digital simulator (RTDS) is employed for modeling of the microgrid. The RTDS is a commercial power system simulator capable of real-time operation, and is widely used in the electric power industry by utilities, equipment manufactures and research organizations [12]-[15]. The RTDS hardware is digital signal processor based and uses a customized parallel processing architecture that designed specifically to solve the electromagnetic transient simulation algorithm. The RTDS software includes a comprehensive library of both power system and control components, and the graphical user interface known as RSCAD [16].

A RTDS-based HIL microgrid testbed for testing, verification, and assessment of microgrid operation and control system has been proposed in this paper. First, the microgrid

This manuscript has been authored by UT-Battelle, LLC under Contract No. DE-AC05-00OR22725 with the U.S. Department of Energy. The United States Government retains and the publisher, by accepting the article for publication, acknowledges that the United States Government retains a non-exclusive, paid-up, irrevocable, world-wide license to publish or reproduce the published form of this manuscript, or allow others to do so, for United States Government purposes. The Department of Energy will provide public access to these results of federally sponsored research in accordance with the DOE Public Access Plan(http://energy.gov/downloads/doe-public-access-plan).

978-1-4673-7151-3/15/$31.00 ©2015 IEEE

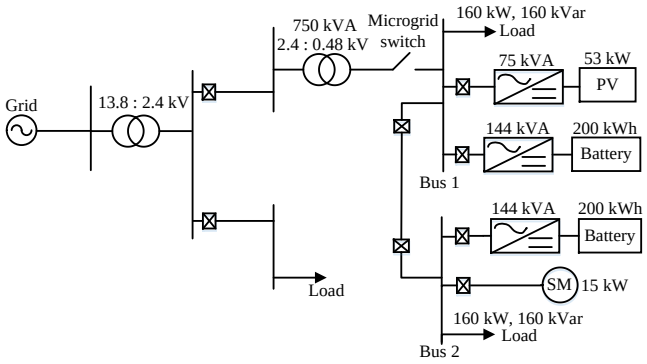

Fig. 1. The diagram of the microgrid.

model and HIL testbed configuration are introduced. Then the applied control system, including the device level control and the microgrid energy management system, is discussed. Finally, testing results are provided to demonstrate the functionality of the HIL microgrid testbed.

II. MICROGRID HIL TESTBED

A. *Microgrid System Description*

A simplified circuit diagram of the microgrid is shown in Fig. 1. The microgrid is connected to local grid (three-phase, 0.48 kV) via a microgrid switch. The microgrid system is composed by two three-phase DC/AC power electronics converters of 144 kVA, one three-phase DC/AC power electronics converter of 75 kVA, two battery systems of 200 kWh, one PV array of 53 kW, one synchronous machine of 15 kW, and two programmable loads of 160 kW, 160 kVar. The PV array is connected to the DC side of the inverter of 75 kVA and then connected to the grid. Each energy storage system is connected to a bidirectional inverter of 144 kVA so that the battery can be charged or discharged.

B. *HIL Testbed Configuration*

The RTDS is a high resolution, real time simulation tool, which is aimed at performing HIL testing. It is able to interface with external hardware using different types of I/O cards, and has real-time response for closed-loop testing such as DER and microgrid controls, protection relay response and coordination, and power electronics controls. Thus, the simulation of control system, communication network, and protection of microgrid with real hardware and Power HIL simulation can be realized. The RTDS-based HIL microgrid testbed is presented in Fig. 2. It is partially software (the microgrid itself is modeled in the RTDS) and partially hardware (the microgrid operation and control system as well as the relay protection system are implemented in hardware).

The employed RTDS can simulate electrical networks of up to 180 electrical nodes. More than 100 analog and digital I/O channels provide sufficient capability to incorporate external equipment into the real-time simulation. It performs power system simulations with a time step of 50 µs. For controls and power electronics simulations, the RTDS uses a time step of 5 µs. Since the higher resolution is needed for accurate simulation of high switching frequencies and calculations used in the power electronic controls. Simulating power electronics requires special models designed for small time step simulation, all of which must be placed in the small time step subsystem. And a large to small time step transformer is needed to link the two parts of the model. The microgrid model in the RTDS includes system topology, detailed dynamic and transient generation and load models, switchgears, sensors, as well as protection relays. Compared to the hardware configurations, it can be easily updated and expanded to allow for modeling of events in various operation scenarios, which helps to promote the development of microgrid research and reduce deployment cost for new devices and solutions. In addition, severe fault or component failure conditions can be

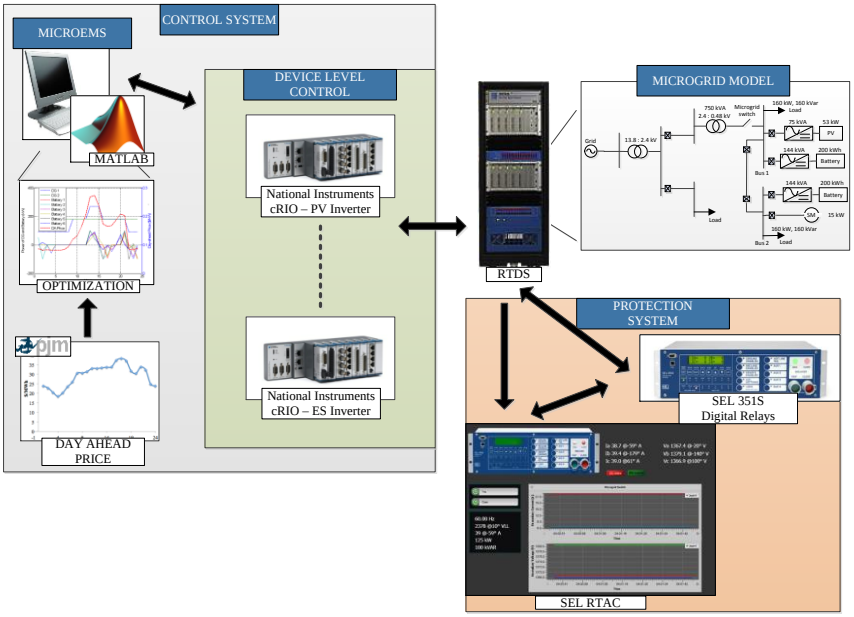

Fig. 2. RTDS-based HIL microgrid testbed configuration.

created and simulated in the RTDS model, and the functionality of the microgrid control and protection system can be evaluated which is difficult or even not feasible in a physical test system.

The conventional computer and NI CompactRIOs 9030 are employed in the HIL testbed as the microgrid control system. The microgrid energy management system (MicroEMS) is implemented by Matlab in the computer. And the device level control, like inverter-based DERs control, load control, is achieved by multiple NI CompactRIOs. Take the energy storage (ES) controller as an example, NI CompactRIO 9030 and I/O modules NI 9220, NI9264 are employed. And the ES controller interface in NI LabVIEW is given in Fig. 3.

Communication between the computer and LabVIEW device level control is performed by using UDP. The presented microgrid controller can be evaluated in the HIL testbed first, and then tested in the corresponding physical microgrid. Actually, the HIL microgrid testbed is aimed at providing a standardized and independent testing. Any developed microgrid controller can be evaluated and tested here by replacing the presented control system and updating the microgrid model in the RTDS.

Meanwhile, to implement fault testing, a relay protection system with a real time automation controller (RTAC) and both virtual and physical relays is added to the testbed. Three SEL 351S programmable digital relays with communication capabilities are applied for selected circuit breakers in the microgrid testbed. They are well suited for overcurrent protection applications. And six setting groups can be predefined and swapped on the fly based on the logic programmed in the relay settings or by external command signals from the RTAC. I/O channels are used to transfer information between the SEL relays and RTDS. SEL relays read CTs and VTs information of the microgrid model from the RTDS through analog channels. SEL relays also read the status of the modeled circuit breakers and control them through digital channels.

The RTAC is a real time operating system with customizable functionality, making it ideal for protection system coordination. In the testbed, the RTAC is interfaced with both the RTDS and SEL 351S relays. The connections with the RTDS are used to monitor the status of circuit breakers and the operational state of the distributed generators. Meanwhile, the RTAC is connected to the relays serially using a proprietary SEL communications protocol for monitoring of relay statuses and measurements as well as centralized control of relay functions.

III. Control System

A communication-assisted hybrid microgrid control and communication architecture [17] has been applied, as shown in Fig. 4. The benefits of both the distributed control and centralized control can be maximized by the three control level design: device level, microgrid control and communication level, and grid level (operation center). The fundamental microgrid functions, including grid-connected and islanding operation, transition between the operation modes, and stable frequency and voltage regulation in islanding mode, will be performed at the device level. The advanced functions are performed by the microgrid control and communication level to achieve the optimal operation of the microgrid: overall system efficiency, DER utilization, reliability, stability, and power quality taking into consideration and constraints.

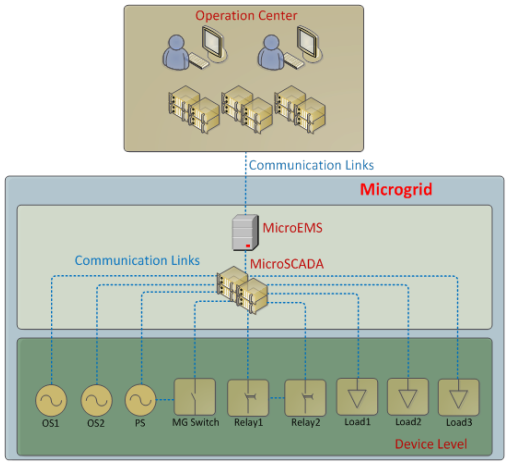

Fig. 4. Microgrid control and communication architecture.

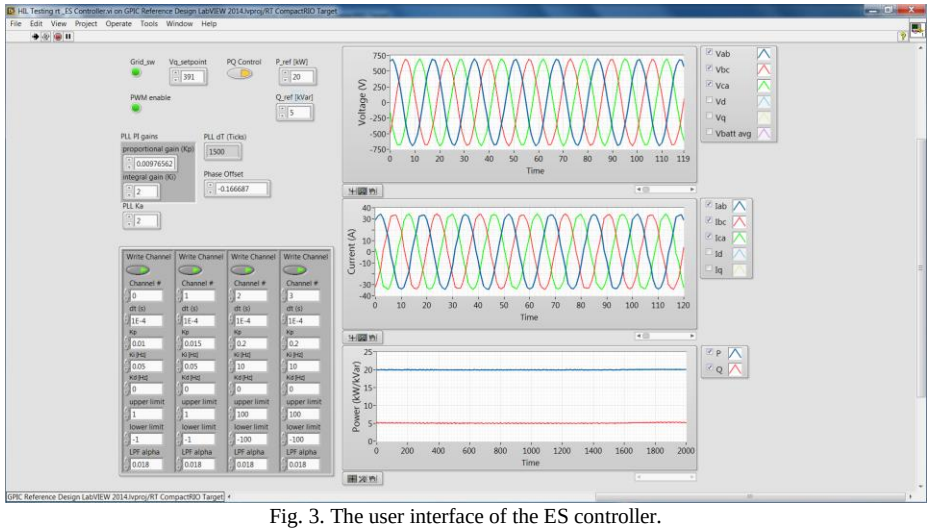
Fig. 3. The user interface of the ES controller.

At the device level, there are three control modes for inverter-based DERs, active and reactive power control, active power vs. frequency (P-f) droop control or reactive power vs. voltage (Q-V) droop control, and frequency or voltage secondary control. Fig. 5 presents the control diagram of active and reactive power control as an example. Open power loop is applied to calculate the active and reactive current reference. The inverter output currents in *abc* coordinates are converted to *dq* coordinates, and regulated through PI controllers to generate the modulation signals. Voltage feedforward control is also added to reduce the inrush current.

The control modes and setting points of each device level controller will be dispatched by the MicroEMS in the microgrid control and communication level. The MicroEMS manages the power flow, power transaction, energy generation and consumption, and battery charging/discharging in the microgrid. The objective is to coordinate among multiple DERs, responsive loads and main grid to improve the system reliability and reduce the total operation cost.

The diagram of MicroEMS is shown in Fig. 6. First of all, the PV power and load for the next 24 hours with 5-minute intervals are forecasted using Artificial Neural Networks. The forecasted data as well as the real-time measurements are utilized by the 5-minute-ahead scheduler to calculate the dispatch orders for all controllable components, such as the control modes and setting points of inverter-based DERs, load adjustments, etc., for the next 24 hours. The optimization problem is formulated as a Mixed Integer Linear Programming (MILP) problem and solved by integer programming function in MATLAB. The 5-minute-ahead scheduler updates the dispatch orders every 5 minutes and only the order for the next 5 minutes are sent to corresponding components.

A microgrid has two operation modes, i.e., grid-connected mode and islanded mode. The operation conditions, system constraints, and operation objectives could be different in different modes. In the grid-connected mode, the MicroEMS

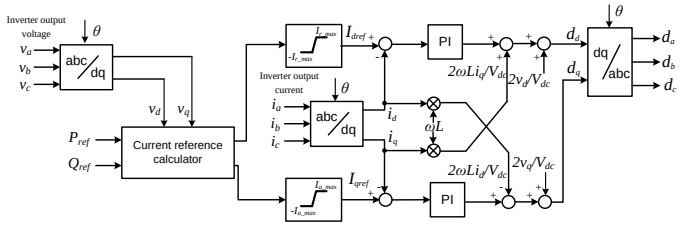

Fig. 5. The control diagram of active and reactive power control.

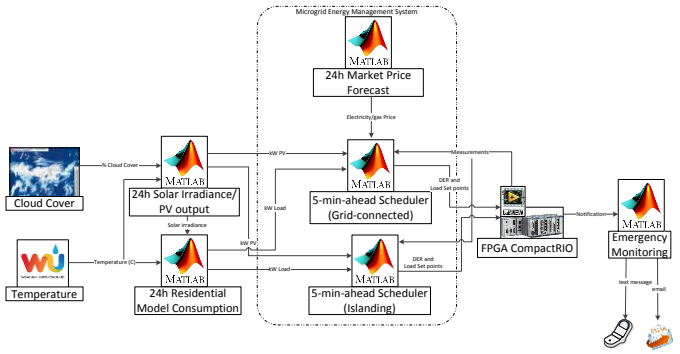

Fig. 6. The diagram of MicroEMS.

communicates with the distribution system, manages the microgrid to comply with the utility policies and minimize the operating cost. In the islanded mode, the primary objectives of the microgrid are to maintain the stability and regulate the voltage and frequency within certain ranges.

IV. Results

The RTDS-based HIL microgrid testbed is designed for testing, verification, and assessment of microgrid components and controllers for system operation, energy management, and protection under different scenarios. Testing results of device level controllers, MicroEMS and the relay protection system are provided to show validation of the proposed HIL system.

A. *Testing of Device Level Controllers*

In this scenario, the PV inverter in bus 1 and the energy storage system in bus 2 are turned on and tested in both grid-connected and islanded modes. As mentioned above, the control system of each inverter has been implemented in the NI CompactRIO 9030 by using NI LabVIEW.

In the grid-connected mode, two inverters are both controlled in the active and reactive power control mode. It should be noticed that the active power control of the PV inverter is different from the scheme shown in Fig. 5. The maximum power point tracking (MPPT) needs to be applied to maximize the solar energy extraction. Thus, an MPPT controller is added to generate the dc-link voltage reference. The voltage of the connected PV array is compared to the voltage reference, and the error is controlled through a PI controller that gives the active current reference.

To show the MPPT function, PV panels are operated under the solar irradiance 600 W/m^2 and temperature 25 ˚C at the begining. And at t = 1s, the solar irradiance increases to 1000 W/m^2. The output power of PV inverter is shown in Fig. 7. It can be seen that the output power is reaching the new maximum solar power 53 kW after 1s. Fig. 8 also gives the PV inverter output current under the irradiance 1000 W/m^2.

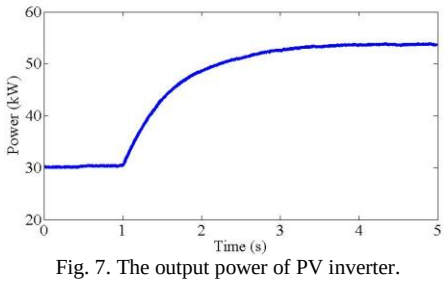

Fig. 7. The output power of PV inverter.

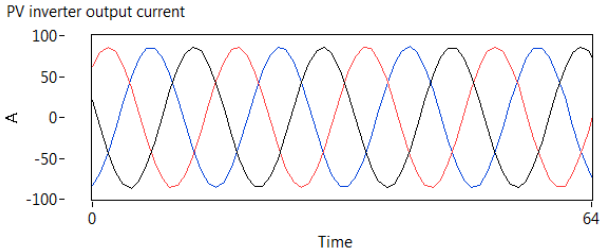

Fig. 8. The output current of PV inverter (under irradiance 1000 W/m^2).

For the energy storage system, the power setting points are P_{ref} = -50 kW, and Q_{ref} = 0, which means the battery is being charged. Then the battery is changed to discharge mode with P_{ref} = 100 kW. The output power and current of the ES inverter are shown in Fig. 9 and 10, respectively.

If the microgrid switch is open, the microgrid will be operated at the islanded mode. The PV inverter is still operated in the power control mode, but the ES inverter is changed to V-f control mode to maintain the voltage and frequency of the microgrid. Fig. 11 presents the output power of the ES inverter during the transition. The load is set as 70 kW and 20 kVar; the reactive power reference of the PV inverter is 10 kVar, and the output active power is 30 kW. When the microgrid switch is open, the control of the ES inverter is changed to V-f mode, and the output power goes to 40 kW and 10 kVar. So that the total power generated by these two DERs is equal to the load consumption. The microgrid voltage during the transition is shown in Fig. 12. The voltage is stabilized in about 1 cycle.

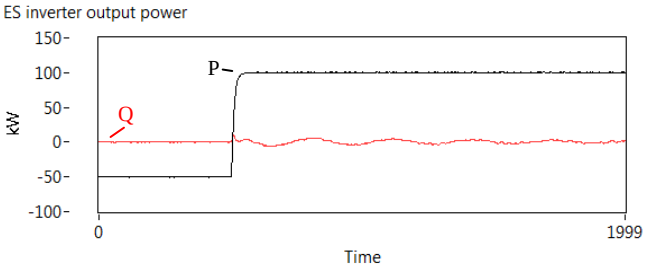

Fig. 9. The output power of ES inverter in the grid-connected mode.

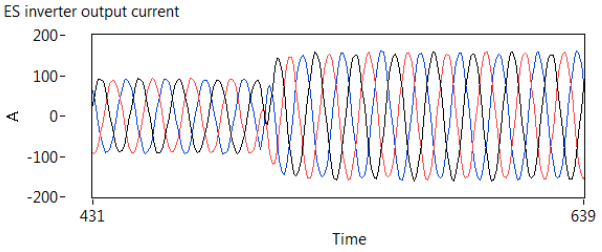

Fig. 10. The output current of ES inverter in the grid-connected mode.

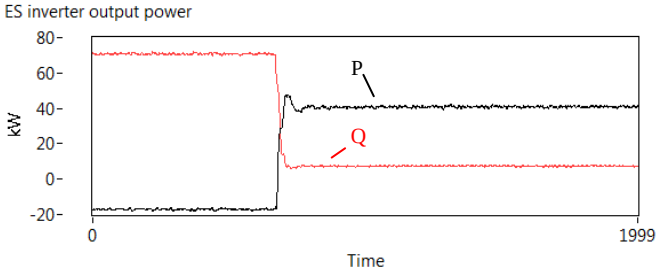

Fig. 11. The output power of ES inverter from the grid-connected to islanded mode.

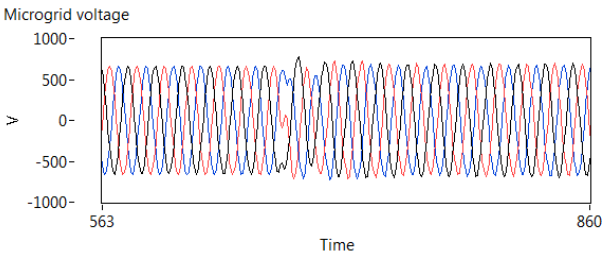

Fig. 12. The microgrid voltage from the grid-connected to islanded mode.

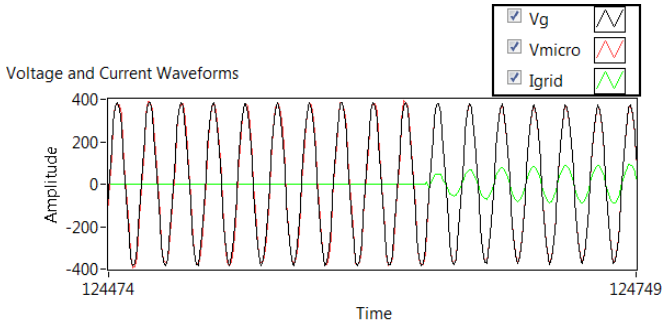

Fig. 13. The voltage and current in phase a during resynchronization.

The voltage and current waveforms in phase *a* during resynchronization is also shown in Fig. 13. If the microgrid is planned to connect back to the grid, the frequency of the microgrid will be controlled to 60.05 Hz, and the magnitude and phase angle of the grid voltage and microgrid voltage will be compared. If the differences are within certain values, the microgrid switch will be closed, as shown in Fig. 13.

B. Testing of MicroEMS

In this scenario, the PV inverter and two energy storage systems are turned on and tested in the grid-connected mode. A load profile emulating the power consumption of 20 houses is sent to control the load in the RTDS microgrid model [18]. The real-time solar irradiance data is also sent to the PV array in the modeled microgrid. The output power of the PV inverter is controlled by the MPPT controller, and setting points of ES controllers are dispatched by the MicroEMS based on its optimization results. In the grid-connected mode, the MicroEMS manages the microgrid to comply with the utility policies and minimize the operating cost.

Fig. 14 presents the testing results of the microgrid testbed in a sunny day from 10 am to 6 pm. The measured powers of the load, PV inverter, two ES systems, and the grid are given, as well as the power setting of two ES systems (shown in black). It can be seen that the measured power of ES systems matches the power reference well. In the afternoon, when both the load power and electricity price are high, the ES systems will be discharged to minimize the operation cost. During that time, the grid power is negative, and the microgrid is sending power back to the grid. In addition, the reactive power compensation is applied for the voltage support in the microgrid.

The testing results in a pretty cloudy day are shown in Fig. 15. The power generated by the PV inverter is much lower. It

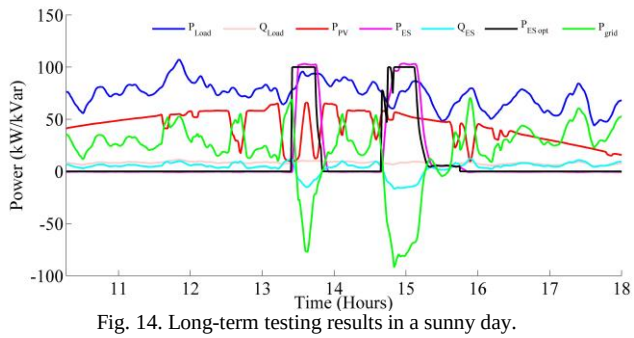

Fig. 14. Long-term testing results in a sunny day.

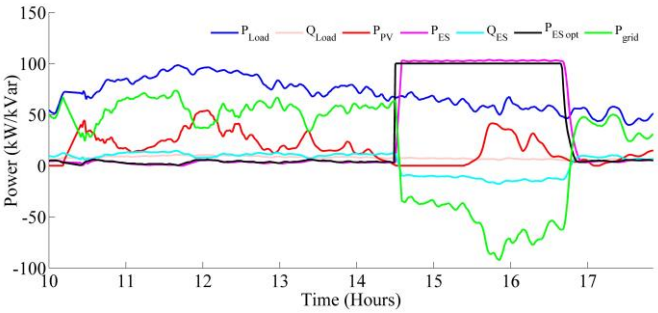

Fig. 15. Long-term testing results in a cloudy day.

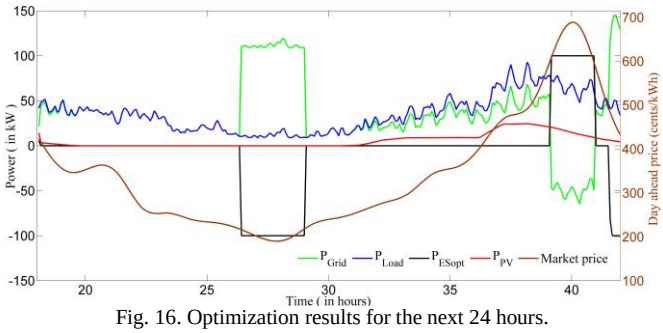

Fig. 16. Optimization results for the next 24 hours.

is even raining between 2:30 pm to 3:20 pm, and the PV inverter is turned off during that time. According to the optimization results, the ES systems are being discharged from approximately 2:30 pm to 4:50 pm. The optimization results of active power at 6 pm for the next 24 hours are also given, as shown in Fig. 16. The ES systems will be charged during the midnight considering both load power and the electricity price. It should be noticed that the results will be updated every 5 minutes and only the orders for the next 5 minutes are sent to corresponding components.

C. Testing of Relay Protection System

To test the relay protection system, the energy storage systems on both buses are turned on, and three-phase fault and single-phase fault are created in the RTDS microgrid model. Different protection schemes can be tested. In the paper, selected testing results of the conventional un-directional overcurrent protection and differential protection are provided.

First, a single setting overcurrent scheme using a time overcurrent characteristic and no directional control is tested. This scenario is analogous to converting a portion of a distribution system into a microgrid without considering protection modifications. In this case the protection is set for the expected utility fault current. Since only three SEL relays are available in the HIL testbed, other relays are modeled in RSCAD. The tested microgrid in RSCAD is shown in Fig. 17, and relay settings are shown in Table I.

To test this protection scheme, faults are applied on each of the two buses in the microgrid and the cable between the two buses as well as a bus outside the microgrid. Three phase faults are applied by inserting an extremely small resistance between the lines and ground, and the response times of the relays are measured. The results are shown in Table II.

In on grid status, external faults are not detected by relay 1

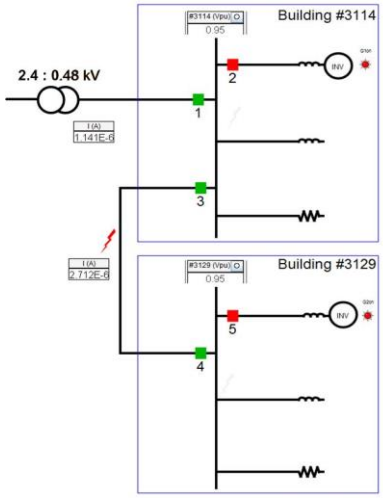

Fig. 17. Microgrid model in RSCAD for protection testing.

TABLE I. OVERCURRENT RELAY SETTINGS

Relay #	Curve Type	Physical Relay?	I_{pickup}	TD
1	U4	Y	12.0	4.0
2	U5	Y	3.0	0.75
3	U4	Y	12.0	2.52
4	U4	N	12.0	1.25
5	U5	N	3.0	0.75

TABLE II. OVERCURRENT PROTECTION OPERATING TIMES

3 Phase Fault		Protection Operation Delay (Cycles)				
Status	Location	Relay #1	Relay #2	Relay #3	Relay #4	Relay #5
On Grid	External	-	14.6	-	-	16.4
	Bus 1	22.1	15.7	-	-	15.7
	Bus 2	-	-	-	15.1	15.3
	Between Buses	-	-	18.5	-	16.2
Islanded	External	-	-	-	-	-
	Bus 1	-	14.0	-	-	15.0
	Bus 2	-	14.1	-	-	15.1
	Between Buses	-	14.2	-	-	15.2

since it is set in anticipation of the large fault current provided by the utility but only measures the fault current produced by the DERs. When the fault is applied to bus 1, relay 1 can observe the utility fault current and operate. Relay 3 and 4 fail to operate in both the on and off grid cases since they only observe the DER fault current. For a normal distribution system, only operating the breaker upstream from the fault would be adequate. However, in the microgrid where DERs are present, it is preferable for relay 3 to operate so that bus 2 can remain in operation. Only a fault applied to bus 2 while on grid can be isolated well from the rest of the system. It can be observed that this conventional un-directional overcurrent protection scheme is not effective, especially when the microgrid is islanded.

An overcurrent based differential scheme is also tested. Appropriately choosing CT polarities and wiring multiple CTs together creates a differential protection that makes use of overcurrent relays. During normal operation, no differential current will be observed by the relays, allowing a very low current pickup to be selected. This protection scheme is

TABLE III. DIFFERENTIAL OVERCURRENT PROTECTION OPERATING TIMES USING SHORT-TIME (U5) CURVE

3 Phase Fault		Protection Operation Delay (Cycles)				
Status	Location	Relay #1	Relay #2	Relay #3	Relay #4	Relay #5
On Grid	External	-	19.8	-	-	22.7
	Bus 1	3.3	3.3	3.3	-	-
	Bus 2	-	-	-	4.2	4.2
	Between Buses	-	-	3.9	3.9	-
Islanded	External	-	-	-	-	-
	Bus 1	-	3.7	3.7	-	-
	Bus 2	-	-	-	6.0	6.0
	Between Buses	-	-	5.7	5.7	-

insensitive to faults outside the protection zone, so there is no need to coordinate with other protections. Thus, the minimum time dial setting or even an instantaneous characteristic can be selected, and internal faults can be cleared quickly.

The testing results of applying three phase faults are presented in Table III. All overcurrent characteristics are set to their minimum settings, 0.25 A pickup current and 0.5 s time dial. It can be seen that three-phase faults are successfully cleared for all locations inside the microgrid in both the grid-connected and islanded modes. However, this test does not offer a solution for isolating the microgrid from external faults.

As an example, Fig. 17 provides the testing result of the differential protection when the microgrid is islanded and three-phase fault is applied on the cable between two buses. After 5.7 cycles, relay 3 and 4 are tripped (shown in green color), leaving bus 1 and 2 still in operation.

V. CONCLUSIONS

A RTDS-based HIL microgrid testbed has been proposed to test operation and control functions of microgrid. It is composed of a RTDS for modeling of the microgrid, a control system including device level control and MicroEMS, and a relay protection system. The microgrid testbed has been tested in the grid-connected and islanded modes as well as resynchronization to verify the fundamental microgrid functions. The MicroEMS and protection system have also been tested in different scenarios. Testing results are presented to demonstrate the functionality of the HIL testbed.

The HIL microgrid testbed is aimed at providing a standardized and independent testing. The presented microgrid model and control system are only examples for the demonstration. Other developed microgrid controllers can also be evaluated and tested on the testbed by replacing the presented control system and updating the microgrid model in the RTDS.

REFERENCES

[1] R. H. Lasseter and P. Paigi, "Microgrid: A conceptual solution," in *Proc. IEEE 35th Annu. Power Electron. Specialists Conf.*, 2004, pp. 4285-4290.

[2] N. Hatziargyriou, H. Asano, R. Iravani, and C. Marnay, "Microgrids," *IEEE Power and Energy Magazine*, vol. 5, pp. 78-94, July/August, 2007.

[3] F. Z. Peng, Y. W. Li, and L. M. Tolbert, "Control and protection of power electronics interfaced distributed generation systems in a customer-driven microgrid," *IEEE Power and Energy Society General Meeting*, pp. 1-8, 2009.

[4] V. Salehi, A. Mohamed, A. Mazloomzadeh, and O. A. Mohammed, "Laboratory-based smart power system, part II: control, monitoring, and protection," *IEEE Trans. Smart Grid*, vol. 3, no. 3, pp. 1405-1417, Sept. 2012.

[5] K. T. Tan, P. L. So, Y. C. Chu, and M. Z. Q. Chen, "Coordinated control and energy management of distributed generation inverters in a microgrid," *IEEE Trans. Power Delivery*, vol. 28, no. 2, pp. 704–713, Apr. 2013.

[6] R. H. Lasseter, J. H. Eto, B. Schenkman, J. Stevens, H. Vollkommer, D. Klapp, E. Linton, H. Hurtado, and J. Roy, "CERTS Microgrid laboratory test bed," *IEEE Trans. Power Delivery*, vol. 26, no. 1, pp. 325-332, Jan. 2011.

[7] B. Washom, J. Dilliot, D. Weil, J. Kleissl, N. Balac, W. Torre, and C. Richter, "Ivory tower of power: microgrid implementation at the University of California, San Diego," *IEEE Power and Energy Magazine*, vol. 11, no. 4, pp. 28-32, July 2013.

[8] M. Barnes, A. Dimwas, A. Engler, C. Fitzer, N. Hatziargyriou, C. Jones, S. Papathanassiou, and M. Vandenbergh, "Microgrid laboratory facilities," in *Proc. Int. Conf. Future Power Syst*., Amsterdam, Netherlands, Nov. 16-18, 2005, pp. 1-6.

[9] B. Lu, X. Wu, H. Figueroa, and A. Monti, "A low-cost real-time hardware-in-the-loop testing approach of power electronics controls," *IEEE Trans. Ind. Electron*., vol. 54, no. 2, pp. 919–931, Apr. 2007.

[10] X. Chen and J. Sun, "Characterization of inverter-grid interactions using a hardware-in-the-loop system test-bed," in *IEEE 8th International Conference on Power Electronics and ECCE Asia*, May 2011, pp. 2180-2187.

[11] J. H. Jeon, J. Y. Kim, H. M. Kim, S. K. Kim, C. Cho, J. M. Kim, J. B. Ahn, and K. Y. Nam, "Development of hardware in-the-loop simulation system for testing operation and control functions of microgrid," *IEEE Trans. Power Electron*., vol. 25, no. 12, pp. 2919–2929, Dec. 2010.

[12] M. Halonen, S. Rudin, B. Thorvaldsson, U. Kleyenstuber, S. Boshoff, and C. van der Merwe, "SVC for resonance control in NamPower electrical power system," in *Proc. PES Summer Meet.*, 2001, Vancouver, Canada, vol.2, pp. 860-865.

[13] A. Guzman, S. Samineni, and M. Bryson, "Protective relay synchrophasor measurements duting fault conditions," in *Proc. Power Syst. Conf.: Adv. Metering, Prot., Control, Commun. and Distrib. Resour*., Clemson, SC, Mar. 2006, pp. 83-95.

[14] H. Li, M. Steurer, K. L. Shi, S. Woodruff, and D. Zhang, "Development of a unified design, test, and research platform for wind energy systems based on hardware-in-the-loop real-time simulation," *IEEE Trans. Ind. Electron.*, vol. 53, no. 4, pp. 1144-1151, Jun. 2006.

[15] S.-M. Baek, and J.-W. Park, "Nonlinear parameter optimization of FACTS controller via real-time digital simulator," *IEEE Trans. Ind. Appl*, vol. 49, no. 5, pp. 2271-2278, Sept./Oct. 2013.

[16] P. Forsyth, and R. Kuffel, "Utility applications of a RTDS simulator," in *Proc. Int. Power Eng. Conf.*, Dec. 2007, pp. 112-117.

[17] Y. Xu, H. Li, L. M. Tolbert, "Inverter-Based Microgrid Control and Stable Islanding Transition," in *IEEE Energy Conversion Congress and Exposition (ECCE)*, Sept. 2012, pp. 2374-2380.

[18] B. J. Johnson, M. R. Starke, O. A. Abdelaziz, R. K. Jackson, and L. M. Tolbert, "A MATLAB based occupant driven dynamic model for predicting residential power demand," in *IEEE PES T&D Conference and Exposition*, Apr. 2014, pp. 1-5.